34th CIRP Design Conference

Design and manufacturing of integrated fluidic channels in glass parts by vat-photopolymerization additive manufacturing

Sijia Liu[a],*, Christoph Klahn[b]

[a]*Karlsruhe Institute of Technology, IMVT Institute for Micro Process Engineering, Hermann-von-Helmholz-Platz 1, 76344 Eggenstein-Leopoldshafen, Germany*
[b]*Karlsruhe Institute of Technology, MVM Institute of Mechanical Process Engineering and Mechanics, Geb. 30.70, 76131 Karlsruhe, Germany*

* Corresponding author. Tel.: +49 721 608-24117; fax: +49 721 608-23186. *E-mail address:* sijia.liu@kit.edu

Abstract

Accurate manufacturing of integrated small-scale fluidic channels in glass structure is of great importance for chemical flow reactors. Vat-photopolymerization of fused silica glass is one of the most promising additive manufacturing technologies to fabricate such structures. It enables the fabrication of glass in a layer-by-layer manner, employing photocurable resin with glass particle fillers, followed by a subsequent thermal treatment to create transparent, fully dense parts. Due to the presence of solid particles, the dimensional accuracy of parts produced by this process is reduced by light scattering. This particularly affects the feasibility and accuracy of small channels, which limits their application as integrated fluidic channel in flow reactors although fused silica glass has excellent chemical and thermal stability. Appropriate printing conditions and rational design play a vital role in ensuring the accuracy of fluidic channels. In accordance with the principle of progressive complexity, this article presents a method to design and manufacture integrated small-scale fluidic channels in glass structures. The case study representing a complex fluidic channel demonstrates the implementation of manufacture and design parameters in a typical flow reactor unit. This work has great implications for designing integrated fluidic channels using particle filler-based vat-photopolymerization additive manufacturing process.

1. Introduction

Fused silica glass, with its excellent chemical, thermal stability, and its optical transparency, is a very promising material to create flow reactors for small-scale chemical reactions [1,2]. Complex fluidic channels with different geometries and precise channel dimensions that can be integrated into flow reactors are essential, as they allow fine-tuning of process parameters such as flow rate, mixing ratio, residence time and reaction temperature to optimize the reaction output [3]. The fabrication of such reactors with integrated fluidic channels through conventional glass manufacturing methods faces significant challenges. It either requires high temperature melting or casting techniques to produce macroscopic objects or the use of aggressive chemicals to etch detailed features [1,2].

With the development of additive manufacturing (AM) technologies, high-resolution glass structuring can now be achieved by vat-photopolymerization (VPP) technology, in which liquid fused silica nanocomposites are polymerized layer by layer using incident light patterns [1,4]. High-quality fused silica glass can be obtained by subsequential heat treatment steps of debinding and sintering [1]. This approach was first published by Kotz et al. [1]. The nanocomposite consists of photocurable polymer and fused silica nanoparticle fillers, which can be shaped via free-radical polymerization resulting in so-called 'green part' [1]. For the manufacturing of small-scale fluidic channel, 'green part' shaping is the most crucial step in determining their dimensional accuracy. However, in

this fabrication stage, the actual polymerized area may differ significantly from the desired area due to over-polymerization also known as over-curing [5,6].

Over-polymerization results from the excessive exposure of the photocurable resin by incident light [6]. When light interacts with the resin, scattering occurs, resulting in over-polymerization in neighboring regions that should not be exposed and cured [7,8]. The impact of this phenomena is even more pronounced in the presence of solid filler, as the introduction of solid particles enhances the light scattering effect significantly [5,6]. Therefore, precise dimensional control is exceptionally challenging for particle filler-based VPP process, especially when manufacturing small-scale fluidic channels [2].

This paper focuses on developing printing and design parameters progressively that enable producing glass structures with high-precision fluidic channels utilizing particle filler-based VPP AM technology. By implementing the identified parameters, integrated fluidic channels in glass structure can be successfully fabricated, demonstrating its potential for application as flow reactor units.

2. Process chain of vat-photopolymerization AM glass

As illustrated in Figure 1, the entire process chain for vat-photopolymerization of AM glass applied in this study is composed of four steps: 'green part' shaping, post-processing, debinding and sintering.
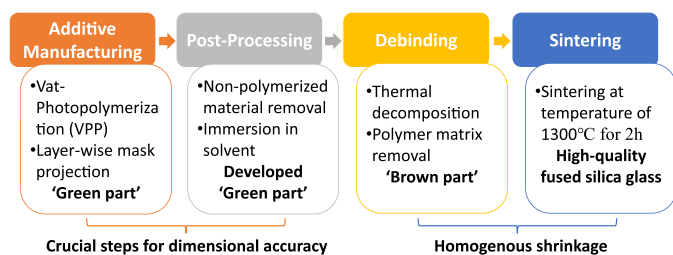
Figure 1. Process chain of vat-photopolymerization of AM glass

The 'green part' shaping process was conducted with a bottom-top additive manufacturing machine ASIGA MAX X27 UV (Resolution: 27 µm, wavelength: 385 nm). It employs digital light processing (DLP) technology to construct projection patterns using a digital micromirror array device (DMDs) to reflect incident light to form a digital mask [9]. The digital model is typically designed using computer-aided design (CAD) software and then sliced into 10 µm to 150 µm thin horizontal cross-sectional layers to form digital black-and-white binary images representing dimensional features of the part at different heights [10]. Using the projection-based light source approach, an entire layer can be selectively cured at once. Each non-black pixel on the layer image is exposed with UV-light and causes a chemical reaction that cures or solidifies the exposed area of the resin [7,10]. The applied UV-curable fused silica glass nanocomposite is the product from Glassomer GmbH called Nanocomposite SL V2.

To obtain fluidic channels with more precise dimensions for a smooth flow of fluids, a solvent called Glassomer Developer produced by Glassomer GmbH was used to achieve a thorough cleaning of the channel.

Thermal treatment steps including 'debinding' and 'sintering' are essentially required. The 'green parts' are heated up stepwise to 600 °C to ensure a complete removal of polymer matrix resulting in so-called 'brown part' (see Supplementary Information) [1]. Afterwards, the 'brown part' is sintered at 1300 °C to get the high-quality fused silica glass [1].

3. Design and manufacturing parameters development for glass structure with integrated fluidic channels

Additive manufacturing is a process of creating three-dimensional objects layer by layer from a digital model [11,12]. For VPP process, the key concept is the sequential projection of two-dimensional patterns onto the surface of the photocurable resin [8,10]. The actual cured area can deviate from the projected pattern because of the volumetric distribution of light, resulting in inaccurate printing [6,10].

Thus, the first prerequisite for ensuring the dimensional accuracy of a fluidic channel is always to analyze the elementary projected elements in a two-dimensional plane and the way the basic projected elements evolve or change during the construction of the 3D model. Subsequently, relevant design recommendations can be developed based on the changes in projection patterns during the 3D construction process and the corresponding interactions between light and materials to achieve the goal of generating complex fluidic channel with high accuracy.

3.1. Simple fluidic channel along z-axis build direction

The simplest fluidic channel is a straight vertical channel of uniform and constant diameter. The influence of AM process parameters on dimensional accuracy and precision is investigated on these channels.

3.1.1. Channel characteristics analysis

When the build direction coincides with the longitudinal axis of the channel, i.e., the angle between the centerline of the channel and the build direction is zero, the basic element of the projection pattern is circle. The same circular pattern will be systematically reproduced along the entire z-axis build direction, as illustrated in Figure 2 a). Since the projection pattern along the build direction is constant, the over-curing could only happen within the xy-plane. The dimensional accuracy of a vertically aligned linear channel mainly depends on the irradiation energy of incident light.

3.1.2. Printing parameters investigation

As illustrated by different authors, the dimensional accuracy of parts produced by particle filler-based VPP AM process strongly depends on the applied irradiation energy [5,6,13,14]. In this study, channel with a design diameter of 1.0 mm was chosen as a representative for investigations and discussions. Ten separate channels with 1.0 mm diameters were designed and incorporated into a 30 mm cylinder to be printed at once, see Figure 2 b).
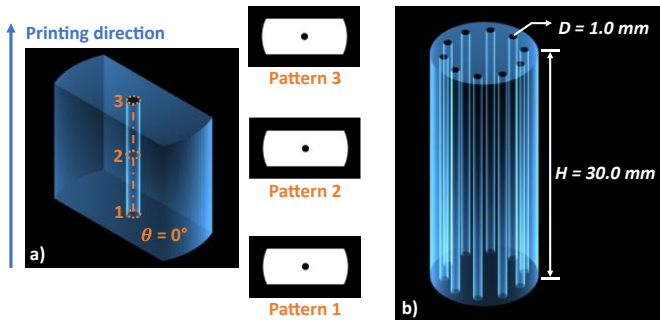
Figure 2. a) Characteristics of simple vertical channel; b) Test cylinder with ten 1.0 mm diameter integrated simple vertical channels

Five different irradiation energies were investigated: 40 mJ/cm², 60 mJ/cm², 80 mJ/cm², 100 mJ/cm² and 120 mJ/cm². At each irradiation energy 3 test cylinder were produced. A layer thickness of 50 μm is suggested by the material supplier.

The measurements of the channel diameter were performed by a light microscope (Olympus SZX12) and the image analysis software OLYMPUS Stream Motion. The mean value and standard deviation of the diameter for 30 channels at each irradiation energy were calculated and presented in Figure 3.

From Figure 3 it can be concluded that, the as-build channel diameter is closely related to the irradiation energy. The higher the applied irradiation energy, the greater the deviation of the printed diameters from the designed diameter and the worse the uniformity of the printed channel. For example, when the applied irradiation energy is higher than 100 mJ/cm², the measured channel homogeneity is extremely poor, showing a strong error bar. This is due to the inhomogeneous over-polymerization caused by strong light scattering effect at high irradiation energy [5,13].

The criterion for proper printing parameter is that the printed channel diameter should be as close as possible to the designed diameter. In addition, the uniformity of the diameter is also of great importance. Considering the distribution of light in z-axis, the irradiation energy should be as low as possible while maintaining smooth printing. This is because when printing complex channels, subsequent light scattering in the z-axis should be avoided if the pattern changes along the build direction. Thus, irradiation energy of 40 mJ/cm² is preferrable
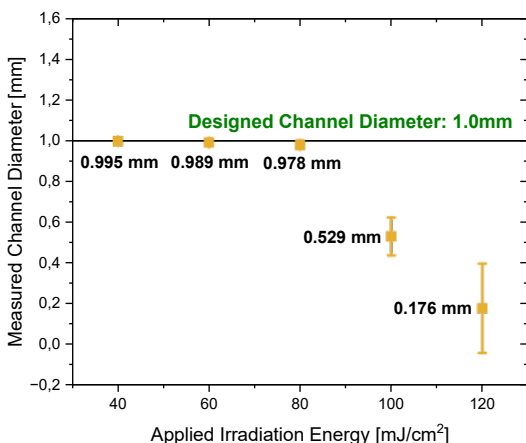
Figure 3. Applied irradiation energy vs. Measured channel diameter

for more precise channel dimensional control. This value will be applied to following chapters for more complex geometries.

3.1.3. Channel diameter after thermal treatments

Thermal treatment consists of debinding and sintering. The brown part after debinding is a fragile, intermediate part, therefore this study focuses on the sintered part. Sintering is the final step in the entire AM glass process chain. During this step, dimensional shrinkage occurs as the particles in the brown part begin to diffuse and bond together [1,6,14]. The voids between the particles are greatly reduced [1,6,14]. Thus, dimensional compensation should always be taken into consideration when designing fluidic channels to be produced by vat-photopolymerization of AM glass.
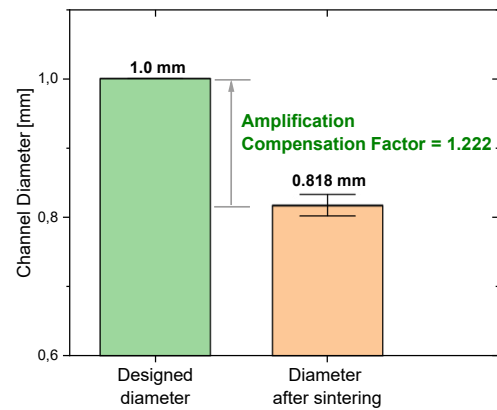
Figure 4. Channel diameter: Design vs. After sintering

Figure 4 shows after sintering at 1300 °C for 2h, in terms of comparing channel diameter 0.818 mm from sintered part directly with the designed diameter 1.0 mm, the design diameter is 1.222 times larger than the actual diameter. This value must be strictly taken into consideration during the design process.

3.1.4. Process parameter recommendations

- Regarding the applied nanocomposite fused silica glass material, 40 mJ/cm² is an appropriate value for small channel fabrication.
- An amplification compensation of 1.222 should be considered during the design process to cope with the shrinkage during the actual sintering process.

3.2. Constrained channel in a two-dimensional plane

Simple vertical fluidic channels with the identical and repeatable circular basic projection patterns were discussed in the previous section. Channels at an angle to the build direction allow the investigation of the influence of process parameters in build direction.

3.2.1. Channel characteristics analysis

If the inlet and outlet of the channel are aligned with the build direction along the z-axis, and the intermediate channel is orientated away from the build direction, the fundamental projection pattern will change. When the channel is constrained
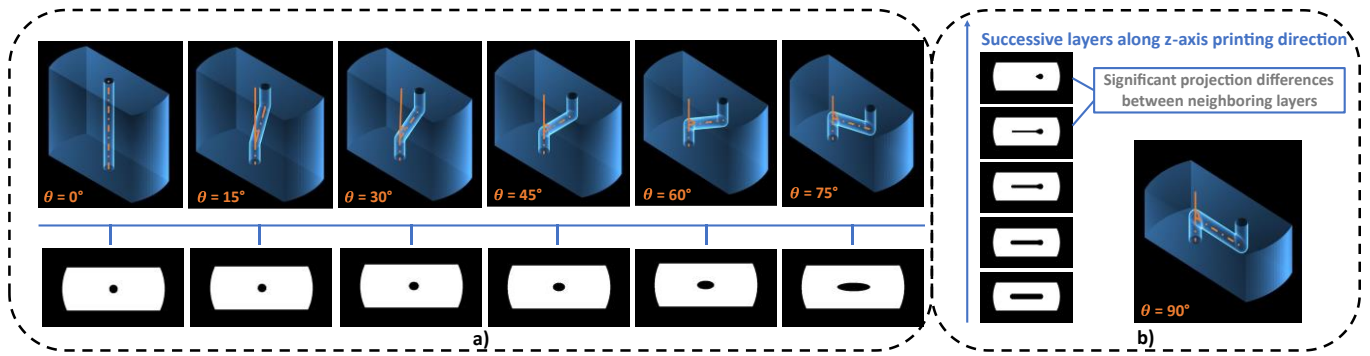
Figure 5. a) Basic projection patterns for different channels in two-dimensional plane; b) Successive projection patterns along printing direction, θ = 90°

to a two-dimensional plane, the angle between the trajectory midline of the intermediate channel and the direction of the AM process plays an important role in the dimensional accuracy.

As the angle increases, the basic projection pattern gradually evolves from a circle to an ellipse. As shown in Figure 5 a), the larger the angle, the greater the eccentricity of the ellipse and the greater the shift between the projection patterns of neighboring layers. More specifically, the angle between the trajectory midline of channel and the printing direction directly correlates with the degree of alteration in the projection pattern.

During the AM process, significant changes in the projection patterns of two adjacent layers can lead to over-curing along the printing direction. More specifically, over-curing in the z-axis direction occurs when the exposed white of the current layer exceeds that of the previous layer and results in a partial overlap with the unexposed black area of the previous layer. An extreme example is when the angle between the centerline of the channel and the z-axis is 90°, the projection patterns of two adjacent layers are almost completely different, see Figure 5 b). In this case, it is practically impossible to generate a fluidic channel with a circular cross-section.

This phenomenon is mainly due to the volumetric distribution of light in the resin [6]. Light energy does not terminate ideally at boundaries of individual layers during the AM process, even though light absorption and scattering within the material causes logarithmic attenuation [10,13]. Instead, the light energy dose is cumulates with each successive layer [10]. Ultimately, this effect can lead to unintended polymerization or gelation in areas that should remain uncured [6,13].

3.2.2. Cross-section evaluation

The cross-section of a channel is defined as the two-dimensional shape that's results from cutting the channel perpendicular to its longitudinal axis. From section 3.2.1, the dimensional accuracy of channel cross-section could be affected by the over-curing effects in z-axis direction. Circularities of cross-sections for channel at different angles were evaluated. The method to calculate circularity was as follows.

The contour of the channel cross-section should first be determined. In equation (1) p_i indicates pixel points on the contour whereby F is the number of contour pixel points. A fitting algorithm is then used to fit a circle to the contour points and the center coordinates of the circle p is found (see Supplementary Information) [15,16].

$$\bar{D} = \frac{1}{F} \sum \|p - p_i\| \qquad (1)$$

$$\alpha^2 = \frac{1}{F} \sum (\|p - p_i\| - \bar{D})^2 \qquad (2)$$

$$C = 1 - \frac{\alpha}{\bar{D}} \qquad (3)$$

Where $\bar{D}$ is the average distance from the pixel point on the contour to the center of the circle. α is the deviation of the distance of the pixel point on the contour to the center of the circle. Circularity C is then calculated using the parameter $\bar{D}$ and α.

Figure 6 shows how normalized circularity (C) varies with the angle (θ) between the trajectory midline of the intermediate
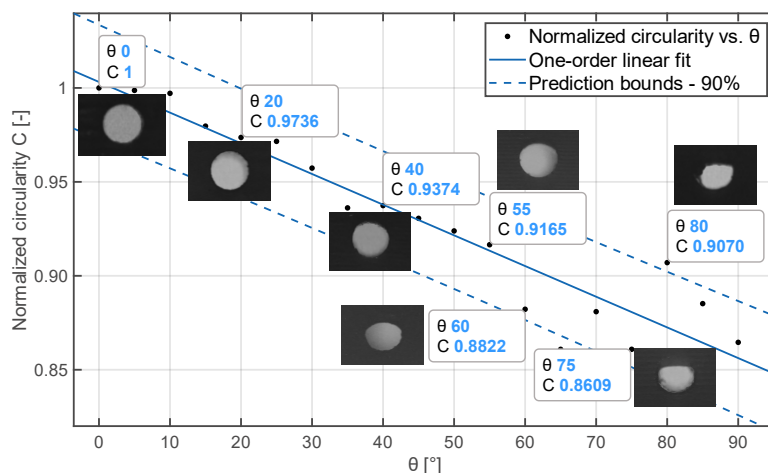
Figure 6. Normalized circularity vs. Angle between the trajectory midline of the intermediate channel and the build direction

channel and the direction of the printing. Ten channels with identical angle were duplicated, and the average circularity of their ten cross-sections was calculated. In addition, all average circularities were normalized using the average circularity at angle of zero as reference value. This is because when the angle is zero, the channel cross-section is considered as the most perfect cross-section that can be produced by this process.

The data depicted in Figure 6 indicates that as the angle increases, the normalized circularity correspondingly decreases. The fitted curve for the plotted data in this figure shows a first-order linear trend. When the angle reaches 60°, the normalized circularity decreases to less than 0.90. As can be seen from the corresponding cross-section image, the profile of channel cross-section is no longer a circle, which means channels above this angle have lost dimensional accuracy. The average circularity deviates in both directions from the fitted curve. This inconsistent deviation also indicates a loss in precision. Besides, the normalized circularity tends to be far away from the fitted line when the angle is greater than 60° and there are some outliers, e.g. when the angle is 80°. From its cross-section image, there are some residues that were not removed during post-processing. In this case the actual circularity calculated by this method might be not accurate.

3.2.3. Design recommendations

- The normalized circularity of cross-section is negatively correlated with the angle between the trajectory midline of the intermediate channel and the direction of the printing.
- It is recommended to keep the angle below 60° to obtain a relatively accurate and uniform channel.

3.3. Helical structure channel in three-dimensional space

Helical channels are investigated as demonstrator of complex three-dimensional channels.

3.3.1. Channel characteristics analysis

The complexity of a helical fluidic channel is greatly increased compared to a channel that is constrained to a two-dimensional plane. As described in section 3.2.2, the accuracy of channel will be influenced by the angle it deviates from trajectory centerline of channel to the direction of the printing process. The same rule can be applied to complex helical structure. However, a more detailed characteristics analysis of the helical structure is necessary.

The trajectory centerline of helical channel is a helix curve, for which the tangent makes a constant angle with a fixed line. The angle between the tangent of helix and the axis of helix can be defined as helix angle, as illustrated in Figure 7.
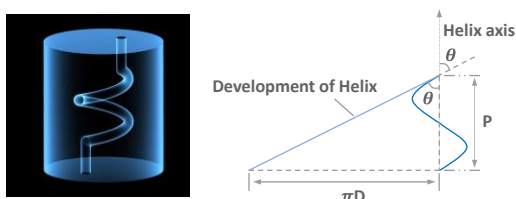
Figure 7. Parameter of helix structure

In the following discussion, only the situation that the axis of the helical structure is aligned with the build direction (z-axis) is taken into discussion. In the terms of helical structure, this angle discussed in section 3.2.2 refers to helix angle θ. In this study, helical structure with a constant helix diameter 5 mm and 4 different pitches were studied, the corresponding helix angles are calculated from equation (4) and summarized in Table 1.

$$\theta = \tan^{-1} \frac{\pi D}{p} \qquad (4)$$

Table 1. Calculation of helix angles θ.

Diameter (mm)	Pitch (mm)	θ
5	16	44.5°
5	12	52.6°
5	8	63.0°
5	4	75.7°

3.3.2. Cross-section evaluation

As illustrated in Figure 8, when helix angle θ is 44.5° and 52.6°, the channel cross-sections are still produced as circles, showing a value of normalized circularity over 0.90. However, when the helix angle further increases to 63.0° and 75.5°, the channel cross-sections loss their dimensional accuracy due to over-curing. This finding is consistent with the observations in the previous section. They indicate that design and manufacturing restrictions investigated on simple parts can be transferred to more complex designs, which was presented by Adam et al. [17] for other AM processes. The present study shows that this approach is applicable to other particle-filler vat-photopolymerization AM process.
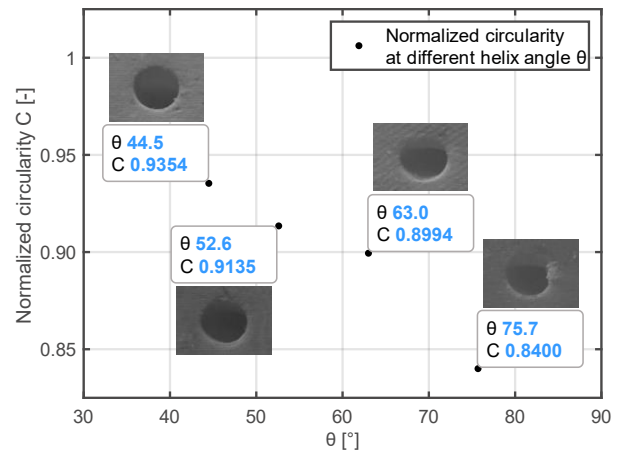
Figure 8. Normalized circularity C at different helix angle θ

3.3.3. Design recommendations

- The angular recommendations for channels in two-dimensional plane can be applied on complex channels in three-dimension.
- Three-dimensional design of integrated fluidic channels can utilize the parameters derived from simpler geometries, to improve the efficiency and the effectiveness of the whole design process.

4. Design case

By implementing the printing and design parameters of this study, it is feasible to fabricate glass parts with integrated fluidic channel in micrometer range. Figure 9 shows a sintered fused silica glass part with integrated fluidic channel derived from the investigated parameters. The integrated channel diameter is 818 μm, which could fulfill typical requirements of micro process engineering reactors. The helical channel represents a feature configuration that can be integrated into a flow reactor system. It could be used either as a cooling channel to control the temperature of the reaction or as reaction channel, where the reaction residence time can be significantly increase with the increment of channel complexity per unit length.
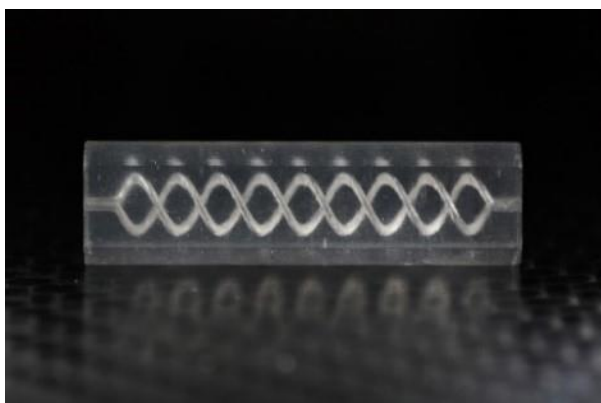
Figure 9. Sintered fused silica glass with integrated helical fluidic channel

5. Conclusion and outlook

The basic scientific approach employed in this study is a systematic progression from elementary conditions and gradually progresses to complexity. The investigation of AM glass structure with integrated fluidic channel consistently involves advancing from simpler geometries to increasingly complex and sophisticated structures. More specifically, simple vertical channels are employed to explore proper process conditions. Subsequently, the possibilities and limitations of additive manufacturing fluid channels under this condition are investigated by gradually increasing the geometric complexity. More complex three-dimensional design of integrated fluidic channels can directly utilize the printing as well as design parameters obtained from simpler geometries. This study demonstrates the feasibility of channels
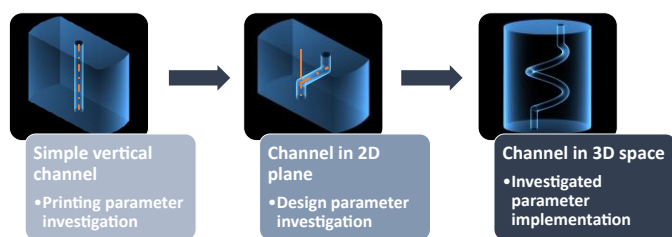
in microfluidic glass parts with a diameter larger than 818 μm at an inclination angle θ smaller than 60°.

The same approach could be transferred to other particle filler-based vat-photopolymerization additive manufacturing process, such as stereolithography ceramic AM process.

Acknowledgements

References

[1]　F. Kotz, K. Arnold, W. Bauer, D. Schild, N. Keller, K. Sachsenheimer, T.M. Nargang, C. Richter, D. Helmer, B.E. Rapp, Three-dimensional printing of transparent fused silica glass, Nature. 544 (2017) 337–339.

[2]　F. Kotz, P. Risch, K. Arnold, S. Sevim, J. Puigmartí-Luis, A. Quick, M. Thiel, A. Hrynevich, P.D. Dalton, D. Helmer, B.E. Rapp, Fabrication of arbitrary three-dimensional suspended hollow microstructures in transparent fused silica glass, Nat. Commun. 10 (2019) 1439.

[3]　M. Baumann, T.S. Moody, M. Smyth, S. Wharry, A Perspective on Continuous Flow Chemistry in the Pharmaceutical Industry, Org. Process Res. Dev. 24 (2020) 1802–1813.

[4]　D. Helmer, B.E. Rapp, Divide and print, Nat. Mater. 19 (2020) 131–133.

[5]　L. Conti, D. Bienenstein, M. Borlaf, T. Graule, Effects of the Layer Height and Exposure Energy on the Lateral Resolution of Zirconia Parts Printed by Lithography-Based Additive Manufacturing, Materials. 13 (2020) 1317.

[6]　S. Zakeri, M. Vippola, E. Levänen, A comprehensive review of the photopolymerization of ceramic resins used in stereolithography, Addit. Manuf. 35 (2020) 101177.

[7]　G. Taormina, C. Sciancalepore, M. Messori, F. Bondioli, 3D printing processes for photocurable polymeric materials: technologies, materials, and future trends, J. Appl. Biomater. Funct. Mater. 16 (2018) 151–160.

[8]　C. Zhou, Y. Chen, Z. Yang, B. Khoshnevis, Digital material fabrication using mask-image-projection-based stereolithography, Rapid Prototyp. J. 19 (2013) 153–165.

[9]　D. Dudley, W.M. Duncan, J. Slaughter, Emerging digital micromirror device (DMD) applications, in: MOEMS Disp. Imaging Syst., SPIE, 2003: pp. 14–25.

[10] E. Guven, Y. Karpat, M. Cakmakci, Improving the dimensional accuracy of micro parts 3D printed with projection-based continuous vat photopolymerization using a model-based grayscale optimization method, Addit. Manuf. 57 (2022) 102954.

[11] ASTM Committee, ISO/TC 261, ISO/ASTM 52900:2021(en), Additive manufacturing — General principles — Fundamentals and vocabulary.

[12] C. Klahn, B. Leutenecker, M. Meboldt, Design Strategies for the Process of Additive Manufacturing, Procedia CIRP. 36 (2015) 230–235

[13] G. Mitteramskogler, R. Gmeiner, R. Felzmann, S. Gruber, C. Hofstetter, J. Stampfl, J. Ebert, W. Wachter, J. Laubersheimer, Light curing strategies for lithography-based additive manufacturing of customized ceramics, Addit. Manuf. 1–4 (2014) 110–118.

[14] T. Chartier, C. Chaput, F. Doreau, M. Loiseau, Stereolithography of structural complex ceramic parts, J. Mater. Sci. 37 (2002) 3141–3147.

[15] T.S.R. Murthy, A comparison of different algorithms for circularity evaluation, Precis. Eng. 8 (1986) 19–23.

[16] L. Xiuming, S. Zhaoyao, Evaluation of roundness error from coordinate data using curvature technique, Measurement 43 (2010) 164–168.

[17] G.A.O. Adam, D. Zimmer, Design for Additive Manufacturing—Element transitions and aggregated structures, CIRP J. Manuf. Sci. Technol. 7 (2014) 20–28.

Figure 10. Method for design and manufacturing of integrated fluidic channels in glass structure by particle filler-based VPP AM process